Trajectory Optimization of a Supersonic Aircraft with a Thermal Fuel Management System

John P. Jasa, * Charles A. Mader, † Joaquim R. R. A. Martins ‡
University of Michigan, Ann Arbor, MI, USA

An aircraft's ability to dissipate heat can have a large impact on its performance. As the complexity and energy usage of next generation aircraft's avionics systems and electrical loads increase, we need to consider thermal effects earlier in the aircraft design process to avoid performance degradation. To do this, we need to consider the interactions between the aerodynamic, propulsive, and thermal systems. This work demonstrates a coupled aero-thermal-mission model which we use to optimize the trajectory of a supersonic aircraft subject to thermal constraints. We show that the optimal flight path depends on the effectiveness of the fuel thermal management system. Introducing a heat exchanger and recirculating warmed fuel back into the tank allowed the aircraft to complete the minimum time-to-climb problem 22 seconds faster than when using a non-recirculating system. We find that for a given heat loading, there exists a trade-off between increasing the thermal capacitance of the aircraft, recirculating fuel, and climbing at a different rate to minimize heat input to the system.

I. Introduction

The goal of aircraft design is to maximize key performance metrics while simultaneously meeting operational and physical constraints. Performance improvements can be achieved by designing a better aircraft or by adding new technologies that enable better performance (e.g., stronger materials, morphing wings). A typical design problem for a military fighter jet would be to minimize take-off gross weight (TOGW) subject to mission requirements, radar cross-section, armament capacity, and maneuverability constraints [1]. The armament requirements could include traditional weaponry as well as high-powered energy weapons, both of which need a sophisticated avionics suite including high-powered radars and significant on-board computing power. In order to function properly, the avionics systems need to be kept below a relatively low temperature of about 100° C, which means that cooling system is needed. The impact of thermal requirements is already apparent in the current generation of fighter aircraft. For example, the F-35 joint strike fighter suffers from thermal management challenges that impact its performance and can require changes to mission profiles to keep temperatures within acceptable ranges [2].

One option for the cooling system is to use fuel-to-air heat exchangers to dissipate heat [3]. This solution tends to interfere with the stealth properties of the airframe and thus may not be a feasible option in modern fighter design. Other solutions have been proposed using fuel thermal management systems (FTMS) to reject waste heat from the aircraft while still maintaining a lower infrared signature [4]. A simple but low efficiency FTMS concept would be to simply dump fuel overboard after it has been used to pick up waste heat, but Alyanak and Allison [5] showed that this would result in a massive increase in TOGW. More refined concepts include using feed tanks and valves to control the fuel cooling loops and then recirculate the hot fuel back into the fuel tank [6]. This approach works as long as the fuel temperature in the tank does not exceed a certain threshold, but for longer missions; the temperature of the fuel in the tank can become a limiting factor.

Another option is to modify the aircraft's trajectory to reach cooler air at higher altitudes where more effective heat rejection is possible through the larger difference between ambient and aircraft temperatures. This has the benefit of improving the effectiveness of the FTMS, but it could also mean that the aircraft is forced to climb faster than it would otherwise have, and hence use more fuel to fly its mission.

*Ph.D. Candidate, Department of Aerospace Engineering, AIAA Student Member
†Research Investigator, Department of Aerospace Engineering, AIAA Senior Member
‡Professor, Department of Aerospace Engineering, AIAA Associate Fellow

Regardless of what solution is chosen, the performance of the FTMS becomes a fundamentally path-dependent problem when aircraft designers are unable to add sufficient heat rejection capabilities into the airframe. This is because the aircraft's full flight path history impacts the thermal performance at any given time. Although path-dependent performance is not typically analyzed as part of early aircraft design, some have considered thermal effects of engines across a flight path, FTMS of aircraft, or thermal history of high-altitude balloons [7, 8].

Considering path-dependent effects as part of an aircraft design process significantly increases the size of the design space via the addition of multiple time-dependent controls that must be optimized along with the physical design characteristics of the aircraft. Given the large design space and highly coupled nature of the design problem, we choose to use gradient-based optimization with analytic derivatives because it offers the most efficient means to finding an optimal solution [9, 10]. Recent work by Falck et al. [11] used gradient based optimization with a pseudo-spectral collocation method for trajectory analysis to find thermally constrained optimal trajectories for NASA's all-electric X-57 X-plane concept. Hendricks et al. also used a pseudo-spectral collocation approach to find optimal minimum time-to-climb trajectories using an aircraft model that integrated a full one-dimensional thermodynamic cycle analysis directly into transient aircraft analysis [12].

The recent work applying pseudo-spectral collocation approach to find optimal trajectories using complex multidisciplinary aircraft models motivates the usage of the same approach for the work presented in this paper. We examine the impact of thermal constraints on the minimum time-to-climb problem for the efficient supersonic air vehicle (ESAV), a representative military fighter aircraft concept. Our aircraft model includes aerodynamic data generated using Reynolds-averaged Navier–Stokes (RANS) computational fluid dynamics (CFD) aerodynamic models, propulsion data generated using one-dimensional thermodynamic models of the F110 turbojet engine, and a transient FTMS system that tracks the temperature of the fuel in the tank. The model is built using NASA's OpenMDAO framework, which facilitates the computation of the derivatives required for the gradient-based optimizer [13]. Although the ESAV aircraft has been optimized before using multidisciplinary design optimization (MDO) with a variety of disciplines, including aerodynamics, structures, stability, mission, noise, and emissions [1, 14, 15, 16], this is the first study of path-dependent problems using thermally-constrained optimal trajectories for the aircraft.

In this work, we construct an aero-thermal-mission coupled model and solve a series of MDO problems to find the optimal trajectory subject to thermal constraints under various heat loadings. We first explain the details of the disciplinary models that comprise the coupled system, then present seven different optimization cases and compare their results.

II. Methodology

To handle the fully coupled system needed to perform aero-thermal-mission MDO, we need an efficient computational framework. We use NASA's OpenMDAO [13, 17, 18] as the underlying framework because of its modularity and derivative-focused data-passing capabilities. OpenMDAO uses the modular and unified derivative (MAUD) [10] theory to calculate the total derivatives of the optimization objective with respect to the design variables. Section III.A expands on the number and types of design variables and constraints for an example optimization problem. The following subsections go into detail about each of the individual disciplinary models and analyses.

A. Atmospheric model

To obtain the air properties at a given altitude, we use the US Standard Atmosphere 1976 tabulated data [20] to create a smooth one-dimensional surrogate model we query during the optimization. We use air temperature, pressure, density, and speed of sound at a given altitude for this work. Because we use Akima splines [21], the surrogate model is smooth and easily differentiable at every point we query.

B. Aerodynamic model — ESAV

The ESAV aircraft provides a common research model for an advanced military fighter aircraft configuration [14, 16]. To obtain the aerodynamic properties of the aircraft, we built a RANS CFD model of the aircraft, which we evaluated at a range of different flight condition to generate an aerodynamic surrogate model. In this work, the shape of the aircraft was held fixed, so we do not need to perform physics-based analysis in the loop to update the aerodynamic properties. This greatly reduces the cost of running the optimization.

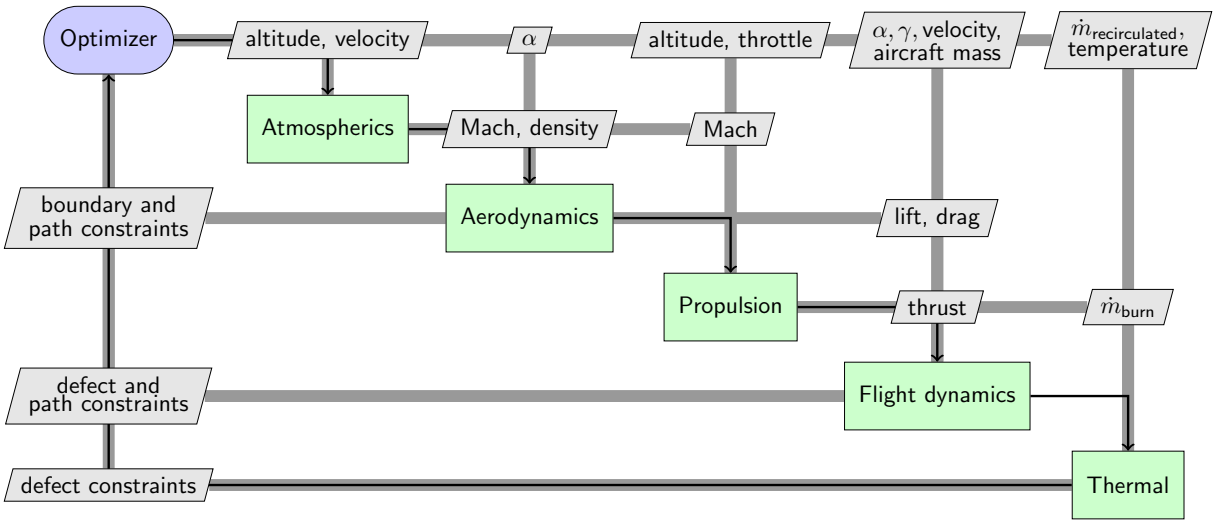

Figure 1. Extended design structure matrix (XDSM) [19] for the multidisciplinary problem.

We began with a CAD surface definition of the aircraft as provided by Lockheed Martin. We plugged the engine inlet and nozzle and removed control surface gaps to simplify the model. These simplifications are possible in this context because we are only considering the aerodynamic properties of the vehicle at different flight conditions without assessing the effects of control surfaces or coupled aeropropulsive effects.

The RANS solver used in this work is ADflow [22, 23], a structured finite-volume CFD code with overset capabilities using an implicit hole cutting scheme [24]. The geometry was meshed using on overset mesh made up of 10 blocks and a total of 2,185,600 cells. This surface mesh and symmetry plane are shown in Fig. 2.

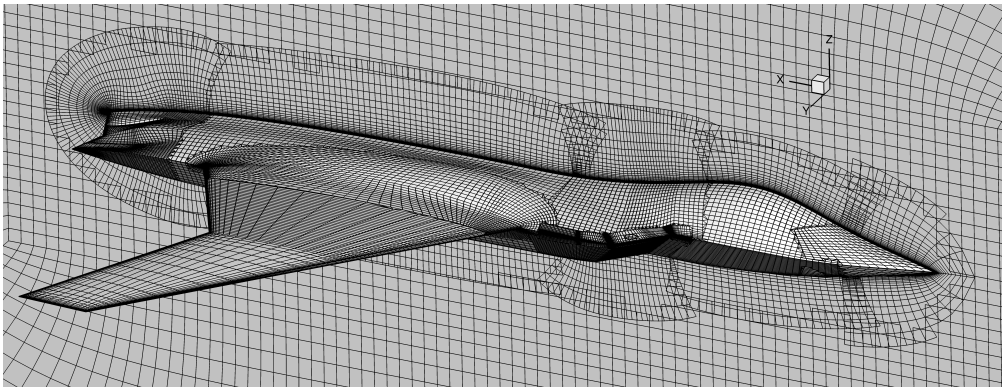

Figure 2. View of the overset mesh used to represent the ESAV geometry. Nine surface patches were created and extruded hyperbolically to create the set of volume meshes.

We converge the flow solution using the approximate Newton–Krylov (ANK) solution algorithm. We use the Spalart–Allmaras turbulence model and the fluxes are discretized with central-differencing. Two nominal flow solutions for the aircraft, one at Mach=0.8 and the other at Mach=1.5, are shown in Fig. 3.

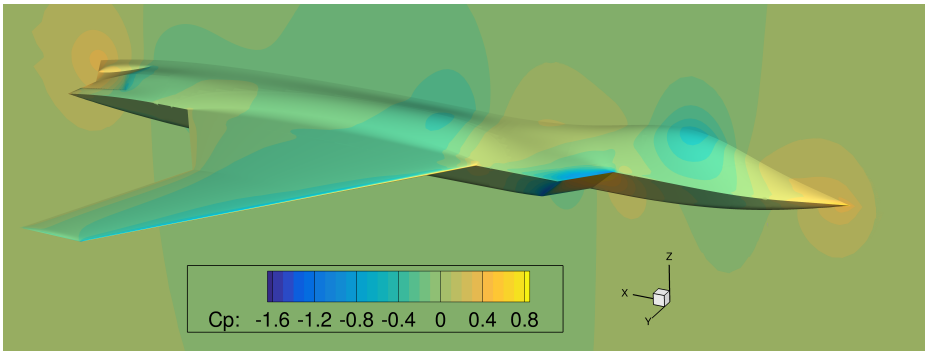

(a) Flow solution at $\alpha = 2$ and Mach=0.8.

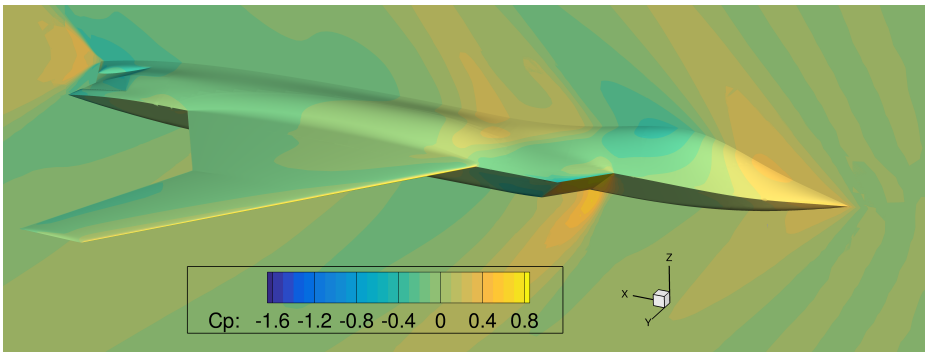

(b) Flow solution at $\alpha = 2$ and Mach=1.5.

Figure 3. Two flow solutions of the ESAV geometry at nominal flight conditions.

Although we could use this CFD model directly in the optimization problem and perform an analysis at each point needed in the mission simulation, we do not need to do that. Instead, we construct a surrogate model based on many training points using data from the CFD analyses. We uniformly query the three-dimensional Mach-α-altitude space to populate the surrogate training points, and obtain C_L and C_D as outputs from the CFD analysis. We use 13 points in the Mach direction, from 0.2 to 1.8, clustered around the transonic region, 7 points from -8 to 8 degrees α, and 3 points in the altitude space between 0 and 20,000 meters for a total of 273 CFD evaluations.

We use this data to construct a surrogate model using the surrogate modeling toolbox (SMT)[a] [25], which provides a variety of methods to represent data sets. We chose to use the energy-minimizing tensor product splines (EMTPS) method [26] because this method has inexpensive training and evaluation costs and also provides gradients of the outputs with respect to the inputs inexpensively. A contour plot of the trained surrogate with the training points overlaid is shown in Fig. 4. Figure 5 shows an angle of attack and Mach sweep of the aerodynamic model at an elevation of 30,000 feet.

C. Propulsion model — F110 engine

We use a surrogate propulsion model based on the GE F110, an afterburning turbofan jet engine. The F110 is a two-spool design with a maximum dry thrust of 16,610 lbf and is used in aircraft such as the F-14 and F-15E [27]. We selected this engine because it is used in aircraft sized similarly to the ESAV aircraft.

To obtain the performance characteristics of this engine, we used a previously developed NPSS model. We ran this model through a corridor of points in the Mach-altitude space with a set of throttles. In all, we ran the model at 152 Mach-altitude combinations and at 8 throttle settings for a total of 1216 evaluated points for the engine model. The outputs we used from this model were thrust and specific fuel consumption (SFC). We then used this data to construct a surrogate model, again using the EMTPS method from SMT. The sampled points and surrogate model contours for a

[a]https://github.com/SMTorg/smt

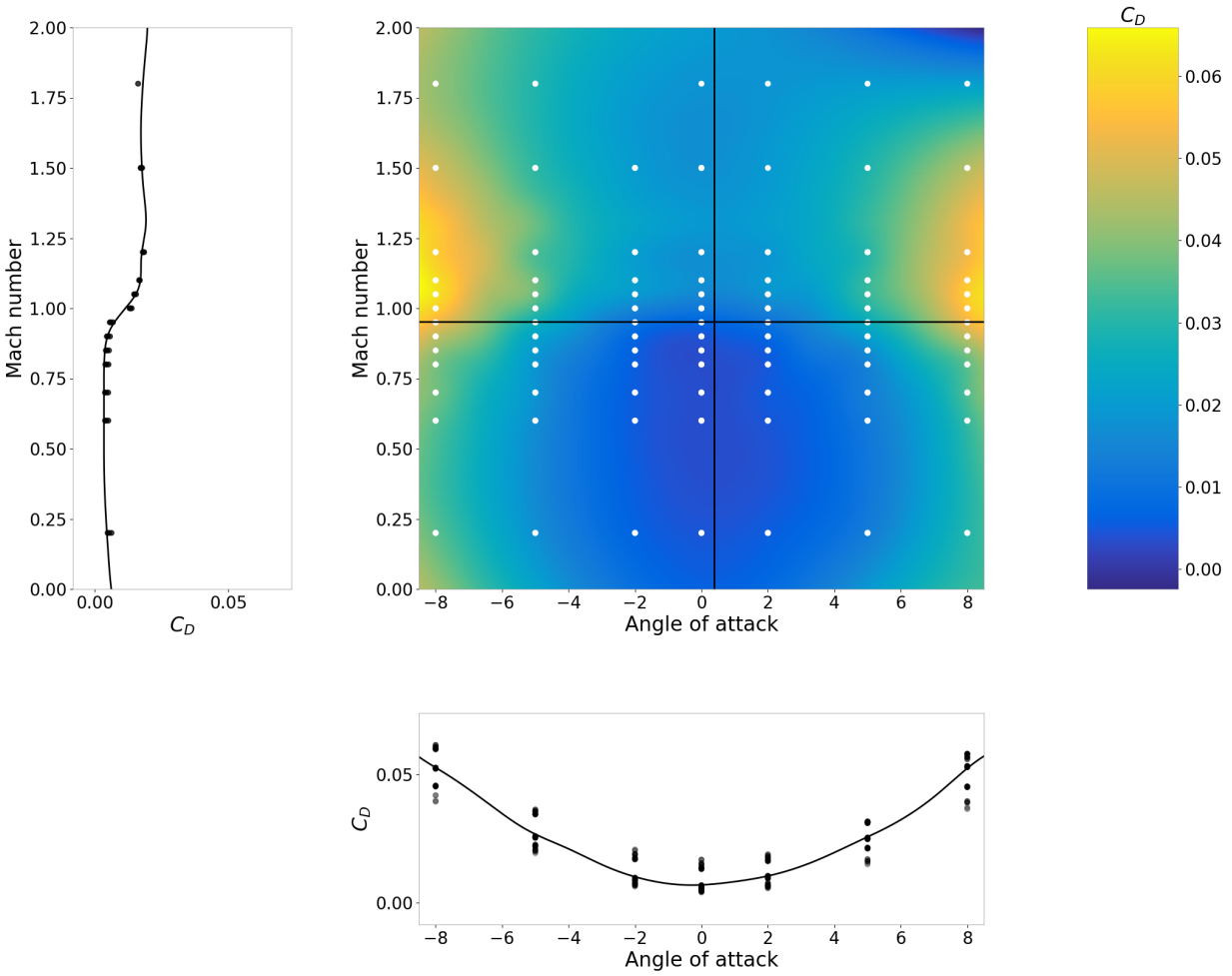

Figure 4. The aerodynamics surrogate model represents the training data well in a smooth and differentiable manner. This plot shows a 2D slice of the 3D input space in the contour and lines, while the points are the training data.

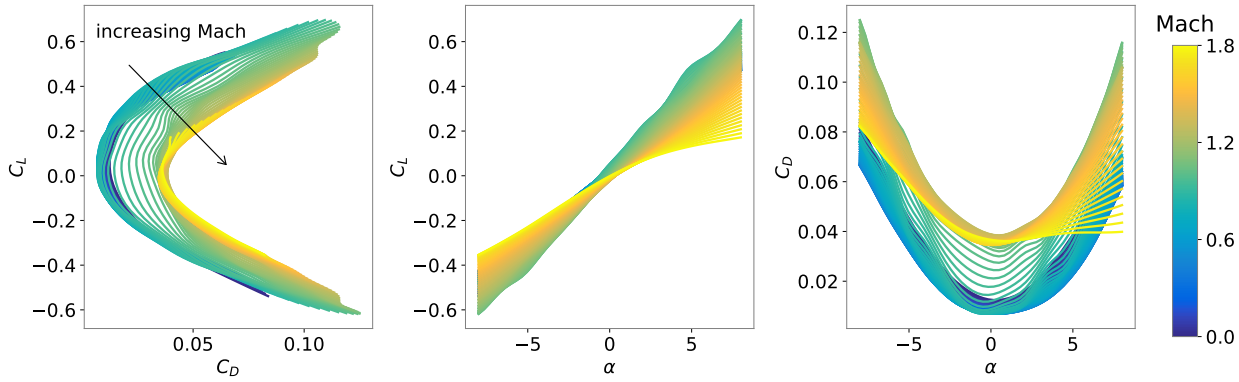

Figure 5. Drag polar and aerodynamic properties for the ESAV aircraft obtained from the CFD-trained surrogate model at an elevation of 30,000 feet with a Mach sweep from 0 to 1.8, and an α sweep from -8 to 8.

throttle setting of 50% are shown in Fig. 6. We found that the surrogate model is smooth and well-behaved throughout the corridor of points, partially due to our ability to run the NPSS model at a large number of conditions.

D. Trajectory model — Dymos

We want to simulate the trajectory of the aircraft in an efficient yet physically realistic manner. We can achieve this by using implicit time integration, such as Legendre–Gauss–Lobatto (LGL) transcription instead of explicitly simulating the trajectory. This allows us to query the aircraft model at fewer points along the trajectory, which makes the overall optimization much less computationally expensive than explicit time integration.

In this work, we use Dymos, a tool developed at NASA Glenn that implements implicit time integration schemes to solve optimal control problems involving dynamical multidisciplinary systems [11, 12]. Dymos uses OpenMDAO and is designed to minimize the effort required to perform multidisciplinary, computationally expensive, or massively parallel dynamical optimization problems. For example, the sparsity structure of the Jacobians in trajectory optimization problems means that we can achieve large increases in derivative computation speed when computing separable constraint derivatives simultaneously.

Determining which ordinary differential equations to solve to determine the aircraft trajectory is not a straightforward process. The most efficient control and state variable formulation is problem-dependent and also requires that the optimization problem is structured correctly for the chosen design space. Here, we use throttle and angle of attack as control variables and range, altitude, velocity, flight path angle, and aircraft mass are states for which the collocation method solves, following a similar procedure as outlined by Falck et al. [11]. This means that we must rearrange the unsteady two-dimensional equations of motion (EOM) for an aircraft to solve for the rate of change in each of these states. Doing this, we obtain

$$\dot{v} = T\cos(\alpha) - Dm - g\sin(\gamma)$$

$$\dot{\gamma} = \frac{T\sin(\alpha) + L}{mv - (g/v)\cos(\gamma)}$$

$$\dot{h} = v\sin(\gamma)$$

$$\dot{r} = v\cos(\gamma),$$

where v is the aircraft velocity, T is the thrust, α is the angle of attack, D is the drag, L is the lift, m is the aircraft mass,

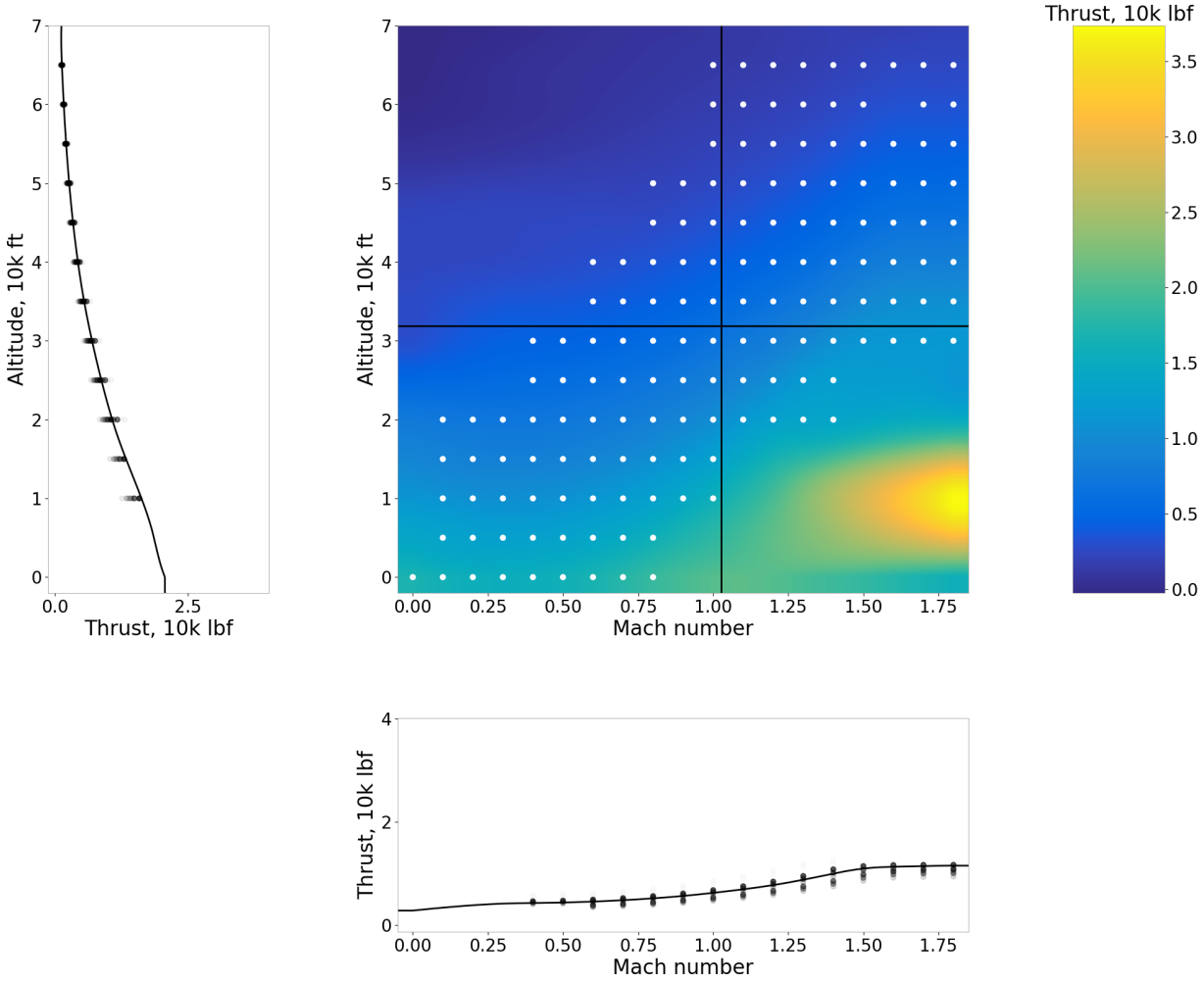

Figure 6. A slice of the propulsion surrogate for a throttle setting of 50%. Although the contour is shown outside of the sample points, the propulsion model is never queried outside the convex region of points.

g is the acceleration due to gravity, r is the aircraft range, and γ is the flight path angle.

Because we selected these EOMs, we have no internal feed-backward coupling (as seen in Fig. 1), which simplifies the analysis and lowers the cost of the optimization. However, this means that some possible analysis points may not be physical, because if the collocation defects are not zero, then the collocation method does not match the actual physics. As the optimizer varies the controls to find the optimal design, it is simultaneously changing the state values at each of the collocation nodes to reduce the state defects to zero, which ensures that the resulting trajectory represents the physics of the system well.

E. Thermal model

For the thermal model, we use a series of equations representing the fuel recirculation FTMS as discussed by Alyanak and Allison [5]. This model consists of a single fuel tank, two heat exchangers, and an engine feed line as shown in Figure 7. The aircraft can dissipate heat generated by on-board electronics or other loads by using the thermal capacitance of the relatively cooler fuel. This FTMS allows heat rejection by burning the heated fuel or by recirculating it back into the fuel tank. The heat removed by the second heat exchanger is represented by $\dot{Q}_{\text{out}}$, but actual aircraft often do not have such an outlet for heat because they are designed to have a minimized thermal signature. Because of that, we consider cases where $\dot{Q}_{\text{out}} = 0$, as well as when we have positive value of $\dot{Q}_{\text{out}}$. There are more complex FTMS architectures to dissipate heat, such as expelling fuel out of the aircraft or having a feed tank, but we only use the recirculation-based method here.

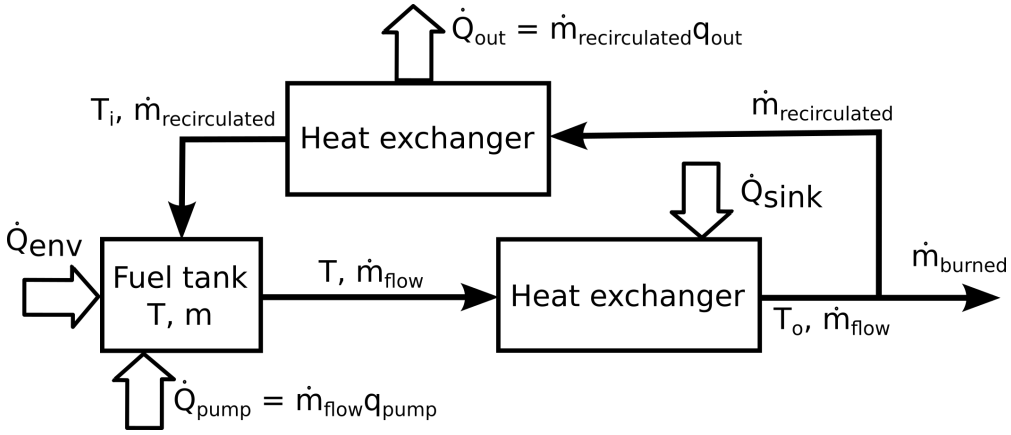

Figure 7. Fuel thermal management system with recirculation used in this work.

For the purposes of this work, we do not consider the length of tubing between thermal components or the time needed for the heat to propagate to the fuel. That is, we assume that heat is instantaneously added and removed from the fuel at the prescribed rates. This allows us to greatly simplify the equations used to describe the state of heat distribution throughout the system.

The original equation relating the rate of temperature change to the heat loads and fuel flow, as presented by Alyanak and Allison [5], is

$$mc_v \frac{dT}{dt} = \dot{Q}_{\text{env}} + \left[1 - \frac{\dot{m}_{\text{burned}}}{\dot{m}_{\text{flow}}}\right] \dot{Q}_{\text{sink}} - \dot{Q}_{\text{out}}, \tag{1}$$

where m is the mass of fuel in the tank, c_v is the specific heat at constant volume, T is the fuel temperature in the tank, $\dot{Q}_{\text{env}}$ is the heat into the tank from the environment, $\dot{Q}_{\text{sink}}$ is the heat from the cooled systems of the aircraft, $\dot{Q}_{\text{out}}$ is the heat removed from the system via heat rejection systems, $\dot{m}_{\text{burned}}$ is the rate of fuel burned, and $\dot{m}_{\text{flow}}$ is the fuel flow rate from the tank.

We use a modified version of this equation that replaces the $\dot{Q}_{\text{out}}$ term with $(\dot{m}_{\text{flow}} - \dot{m}_{\text{burned}})q_{\text{out}}$ to account for the ability for the heat exchanger to remove more heat as the fuel mass flow rate increases. This means we can circulate

more fuel to cool the tank at the cost of added pump heat and energy. Heat can only be removed from this system by burning it or by recirculating through the second heat exchanger. Additionally, we add another heat source that is dependent on the total fuel flow rate in the system. This source is representative of any heating that occurs as a function of fuel flow, thrust generated, or throttle setting, such as waste heat from gearbox bearings and shafts, oil pumps, or geared lift fans. The final equation used to obtain the temperature rate of the tank is

$$\frac{dT}{dt} = \frac{\dot{Q}_{\text{env}} + \dot{m}_{\text{flow}} q_{\text{pump}} + \left[1 - \frac{\dot{m}_{\text{burned}}}{\dot{m}_{\text{flow}}}\right] \dot{Q}_{\text{sink}} - (\dot{m}_{\text{flow}} - \dot{m}_{\text{burned}}) q_{\text{out}}}{m c_v}, \tag{2}$$

where $\dot{m}_{\text{flow}}$ is the total mass fuel flow in the system and q_{pump} is a coefficient that dictates how much heat is added as af unction of that total mass flow.

III. Results

A. Optimization problem formulation

For each result in this paper, we use the same basic optimization problem formulation with modifications for each case. Table 1 shows a nominal optimization problem, where we find the minimum time for the aircraft to climb to 20,000 meters, reach Mach 1, and a horizontal flight path angle. The aero-thermal-mission problem is set up so we can easily change the discretization, choose to optimize the recirculation or not, vary the heat inputs, and many other combinations of settings.

The thermal loads used in each case are based on estimates of next generation fighter jets' avionics, armament, and waste heat generating systems. For all cases in this paper, we use 25 mission segments of transcription order 3 in an LGL scheme. We use an operating empty weight of 10,500 kg and start the mission phase after takeoff. The ambient and starting temperature for the fuel is 310 K and we set a limit of 312 K to represent the maximum temperature rise allowable for this portion of the entire mission. In all cases, we use a gradient-based optimizer, SNOPT [28], through the Python interface pyOptSparse[b] [29].

[b] https://github.com/mdolab/pyoptsparse

Table 1. Nominal optimization problem formulation

Category	Name	Quantity		Lower	Upper	Units
		No recirculation	Recirculation			
Objective	time	1	1	–	–	seconds
Variables	α	50	50	-8	8	degrees
	throttle	50	50	0	1	–
	$\dot{m}_{\text{recirculated}}$	0	50	0	–	kg/s
	range	25	25	0	1000	km
	altitude	25	25	0	20	km
	velocity	25	25	10	–	m/s
	γ	25	25	-86	86	degrees
	mass	25	25	15,000	80,000	kg
	temperature	25	25	–	–	K
	time	1	1	0	–	seconds
	Total	**251**	**301**			
Constraints	final altitude	1	1	20,000	20,000	m
	final Mach	1	1	1.0	1.0	–
	final γ	1	1	0	0	degrees
	Mach	75	75	0.1	1.8	–
	temperature	75	75	–	312	K
	$\ddot{m}_{\text{recirculated}}$	0	24	0	–	$1/s^2$
	$\dot{m}_{\text{flow}}$	0	24	0	50	kg/s
	range defects	25	25	0	0	km
	altitude defects	25	25	0	0	km
	velocity defects	25	25	0	0	m/s
	γ defects	25	25	0	0	degrees
	mass defects	25	25	0	0	kg
	temperature defects	25	25	0	0	K
	$\dot{\alpha}$ defects	24	24	0	0	degrees/s
	throttle rate defects	24	24	0	0	$1/s$
	Total	**348**	**396**			

B. Optimal trajectories under different $\dot{Q}_{\text{env}}$ loads

For the set of optimization cases, we do not allow the optimizer to recirculate any fuel while subjecting the system to a specified heat load through $\dot{Q}_{\text{env}}$ and $\dot{Q}_{\text{sink}}$. This means it must increase the amount of fuel in the tank to increase the thermal capacitance of the system to stay below the temperature limit.

Table 2. Heat loads for results shown in Fig. 8.

	Color	Recirculation	$\dot{Q}_{\text{env}}$, kW	$\dot{Q}_{\text{sink}}$, kW	q_{pump}, kW/kg	q_{out}, kW/kg
Case 1	Blue	No	400	100	0	0
Case 2	Orange	No	450	100	0	0
Case 3	Green	No	500	100	0	0

Figure 8 shows the results from three separate optimization cases, where each has the parameters as described above, but they have different $\dot{Q}_{\text{env}}$ values. The heavier aircraft cannot accelerate as quickly, which means that in the optimal trajectory the aircraft spends more time building up speed near a fixed altitude before climbing to the desired altitude. Case 3 takes 135 seconds to climb while Case 1 only takes 113 seconds. Although this is a fairly straightforward result, it confirms that the fully coupled system and optimization problem behave as expected.

C. Effect of allowing recirculation

We now compare the worst case scenario from Fig. 8 with a case where we allow the optimizer to control the amount of fuel being recirculated throughout the system. Additionally, we set q_{out} to be 5000 kJ/kg, which means that we assume there is a heat exchanger that removes an amount of heat from the fuel dependent on the recirculated mass flow. We limit the total mass flow of the system so that the sum of the mass fuel burn rate and the recirculation rate must be less than or equal to 50 kg/s.

Table 3. Heat loads for results shown in Fig. 9.

	Color	Recirculation	$\dot{Q}_{\text{env}}$, kW	$\dot{Q}_{\text{sink}}$, kW	q_{pump}, kW/kg	q_{out}, kW/kg
Case 3	Green	No	500	100	0	0
Case 4	Red	Yes	500	100	0	5

With the ability for the aircraft to recirculate fuel, the aircraft can climb at a faster rate due to its decreased mass as it needs to carry less overall fuel to cool the system. The amount of fuel being recirculated is such that the total fuel flow is always at the limit of 50 kg/s.

D. Effect of pump-rate-dependent heating

The last set of cases we examine here introduces a thermal term that is dependent on the mass flow rate through the main fuel pump. This heat source is a simplified representation of a variety of heat sources that increase as fuel flow or thrust increase, including waste heat from gearbox bearings and shafts, oil pumps, and geared lift fans. For these cases, we do not have any other sources of heat except the flow-dependent term, and we do not consider any fuel recirculation effects.

Essentially, the optimizer could choose to load more fuel onto the aircraft to increase thermal capacitance, or fly at lower throttle (lower fuel flow rate) to lessen the heat loads. Figure 10 shows the results of the three optimization cases described in Table 4.

We see a drastic difference in the optimal trajectories for each of these cases because the amount of heat being added to the system is dependent on the fuel flow rate, which in turn depends on throttle, altitude, and Mach. When the thermal load is at the worst case scenario, shown in pink, we see the optimizer choose to greatly increase the amount of fuel on-board, but also decrease the throttle setting during the initial portion of the mission. This combination leads to a much longer minimum time-to-climb compared to the two other cases. Each case is thermally constrained here, but the case with the lowest q_{pump} coefficient requires much less fuel to complete the mission. It starts with 7589 kg of fuel compared to the worst case scenario's 16,276 kg. This shows the large effect on sizing that thermal constraints can have, even if we are able to optimize the trajectory simultaneously.

Table 4. Heat loads for results shown in Fig. 10.

	Color	Recirculation	$\dot{Q}_{\text{env}}$, kW	$\dot{Q}_{\text{sink}}$, kW	q_{pump}, kW/kg	q_{out}, kW/kg
Case 5	Purple	No	0	0	200	0
Case 6	Brown	No	0	0	300	0
Case 7	Pink	No	0	0	400	0

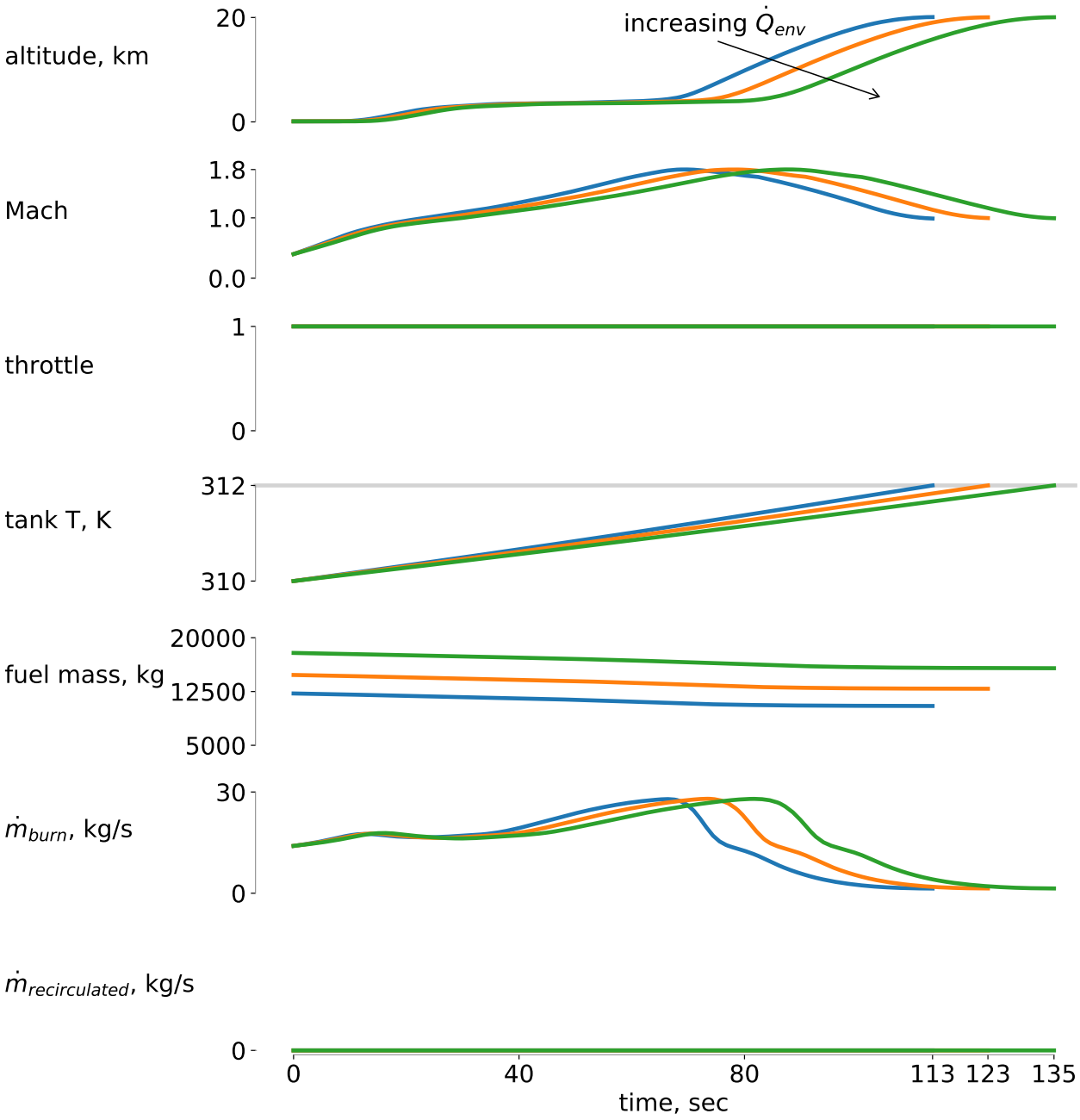

Figure 8. As we increase the thermal load on the fuel tank, we see the trajectories get less aggressive due to the increased aircraft mass.

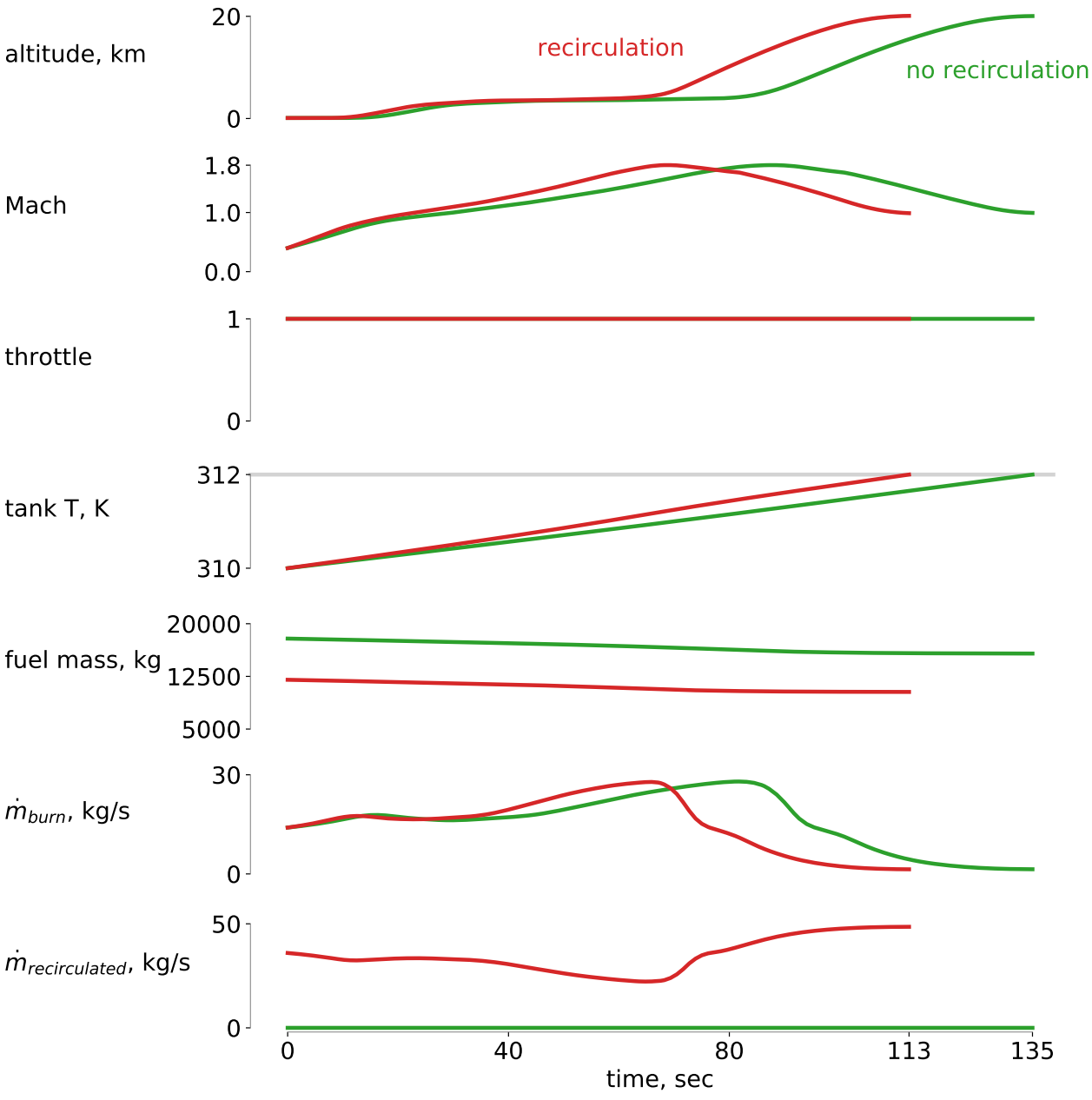

Figure 9. Allowing the FTMS to recirculate fuel to cool down the system yields a minimum time-to-climb that is 22 seconds less than without fuel recirculation.

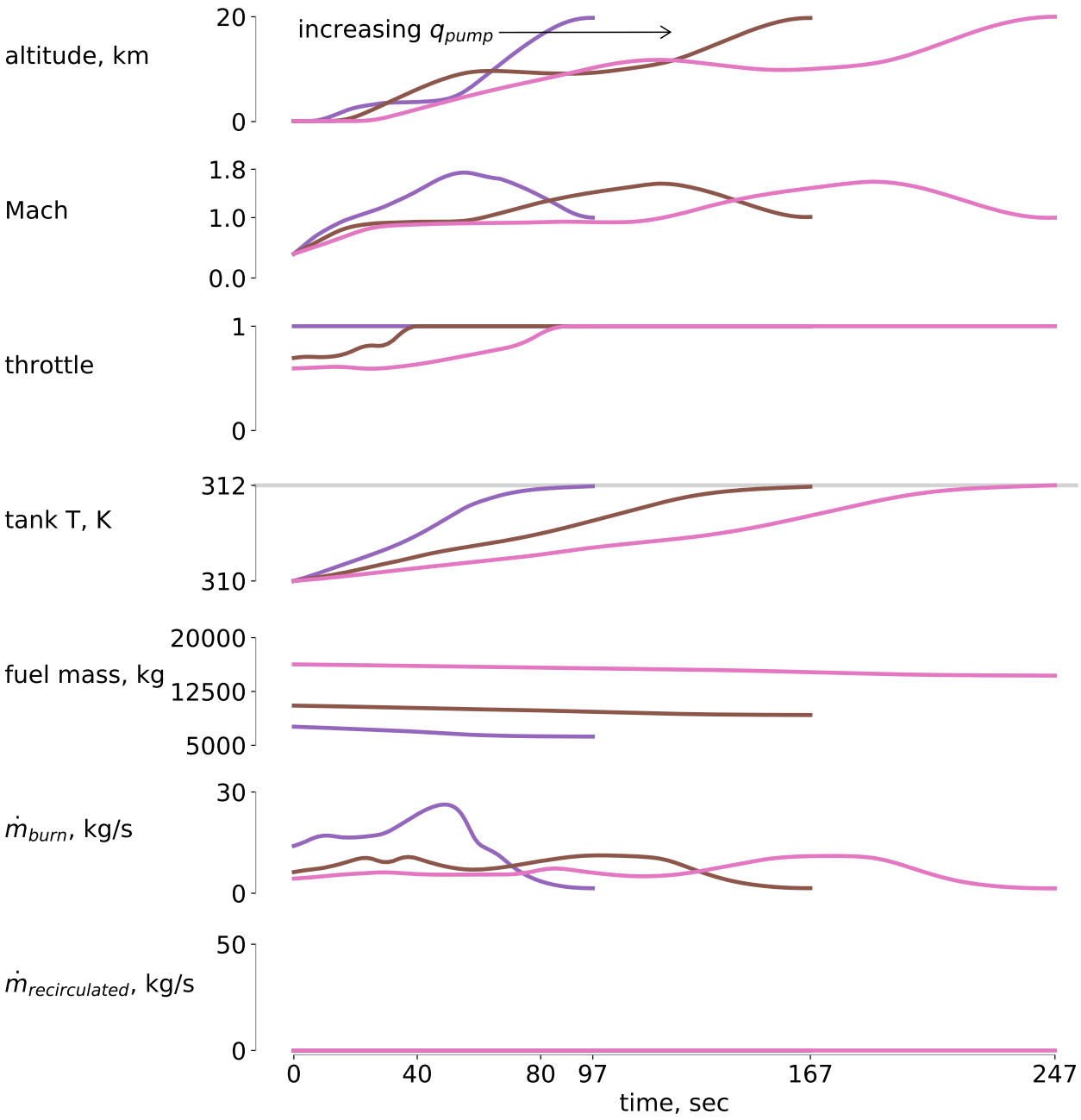

Figure 10. In these cases, we only have one thermal source whose magnitude is correlated to the total fuel flow rate. The optimizer both increases on-board fuel and decreases throttle in the worst-case scenario to stay within the thermal constraint.

IV. Conclusions

We constructed a fully-coupled aero-thermal-mission model to optimize the trajectory of a supersonic air vehicle subject to thermal constraints. We used a RANS CFD-based surrogate model for the aerodynamic analysis, a surrogate model based on one-dimensional thermodynamic cycle analyses for the propulsion, and a transient fuel thermal management system that tracks the temperature of the fuel in the tank across the mission. We can then perform implicit time integration to obtain the aircraft performance across its mission and optimize it based on our defined control and state parameters.

We optimized seven individual cases with varying heat loads and recirculation abilities. These results showed that the heat loads within a supersonic aircraft can affect the optimal trajectory and operating conditions when the aircraft is thermally constrained. Without advanced FTMS or heat rejection capabilities, the aircraft requires additional fuel to increase its thermal capacitance to stay with the thermal constraints, even if we optimize the trajectory and throttle controls. Introducing a heat exchanger and recirculating warmed fuel back into the tank allowed the aircraft to complete the minimum time-to-climb problem 22 seconds faster than when using a non-recirculating system. These results show that the performance of the next generation of fighter jets may be degraded if thermal effects and FTMS are not considered early enough in the design process.

V. Acknowledgements

The first author is grateful for support from the National Science Foundation Graduate Research Fellowship under Grant No. DGE-1256260. This work is supported in part by the U.S. Air Force Research Laboratory (AFRL) under the Michigan-AFRL Collaborative Center in Aerospace Vehicle Design (CCAVD), with Darcy Allison as the task Technical Monitor. The authors thank Justin Gray for many worthwhile discussions on how to approach the coupled problem, Rob Falck for his assistance using the collocation schemes, and Jon Seidel for providing and running the F110 NPSS model.

References

[1] Allison, D., Morris, C., Schetz, J., Kapania, R., Sultan, C., Deaton, J., and Grandhi, R., "A multidisciplinary design optimization framework for design studies of an efficient supersonic air vehicle," *12th AIAA Aviation Technology, Integration, and Operations (ATIO) Conference and 14th AIAA/ISSMO Multidisciplinary Analysis and Optimization Conference*, 2012, p. 5492.

[2] Gertler, J., "F-35 Joint Strike Fighter (JSF) Program," Library of Congress Washington DC Congressional Research Service, 2012.

[3] Huang, H., Spadaccini, L. J., and Sobel, D. R., "Fuel-cooled thermal management for advanced aero engines," *ASME Turbo Expo 2002: Power for Land, Sea, and Air*, American Society of Mechanical Engineers, 2002, pp. 367–376.

[4] Mahulikar, S. P., Sonawane, H. R., and Rao, G. A., "Infrared signature studies of aerospace vehicles," *Progress in Aerospace Sciences*, Vol. 43, No. 7-8, 2007, pp. 218–245.

[5] Alyanak, E. J. and Allison, D. L., "Fuel Thermal Management System Consideration in Conceptual Design Sizing," *57th AIAA/ASCE/AHS/ASC Structures, Structural Dynamics, and Materials Conference*, 2016, p. 0670.

[6] Doman, D. B., "Fuel flow control for extending aircraft thermal endurance part I: Underlying principles," *AIAA Guidance, Navigation, and Control Conference*, 2016, p. 1621.

[7] Carlson, L. A. and Horn, W., "New thermal and trajectory model for high-altitude balloons," *Journal of Aircraft*, Vol. 20, No. 6, 1983, pp. 500–507.

[8] Bodie, M., Russell, G., McCarthy, K., Lucas, E., Zumberge, J., and Wolff, M., "Thermal analysis of an integrated aircraft model," *48th AIAA Aerospace Sciences Meeting Including the New Horizons Forum and Aerospace Exposition*, 2010, p. 288.

[9] Lyu, Z., Xu, Z., and Martins, J. R. R. A., "Benchmarking Optimization Algorithms for Wing Aerodynamic Design Optimization," *Proceedings of the 8th International Conference on Computational Fluid Dynamics*, Chengdu, Sichuan, China, July 2014, ICCFD8-2014-0203.

[10] Hwang, J. T. and Martins, J. R. R. A., "A computational architecture for coupling heterogeneous numerical models and computing coupled derivatives," *ACM Transactions on Mathematical Software*, 2018, (In press).

[11] Falck, R. D., Chin, J. C., Schnulo, S. L., Burt, J. M., and Gray, J. S., "Trajectory Optimization of Electric Aircraft Subject to Subsystem Thermal Constraints," *18th AIAA/ISSMO Multidisciplinary Analysis and Optimization Conference*, Denver, CO, June 2017.

[12] Hendricks, E. S., Falck, R. D., and Gray, J. S., "Simultaneous Propulsion System and Trajectory Optimization," *18th AIAA/ISSMO Multidisciplinary Analysis and Optimization Conference*, Denver, CO, June 2017.

[13] Gray, J., Hearn, T., Moore, K., Hwang, J. T., Martins, J. R. R. A., and Ning, A., "Automatic Evaluation of Multidisciplinary Derivatives Using a Graph-Based Problem Formulation in OpenMDAO," *Proceedings of the 15th AIAA/ISSMO Multidisciplinary Analysis and Optimization Conference*, Atlanta, GA, June 2014. doi:10.2514/6.2014-2042.

[14] Burton, S., Alyanak, E., and Kolonay, R., "Efficient supersonic air vehicle analysis and optimization implementation using SORCER," *12th AIAA Aviation Technology, Integration, and Operations (ATIO) Conference and 14th AIAA/ISSMO Multidisciplinary Analysis and Optimization Conference*, 2012, p. 5520.

[15] Alyanak, E. and Kolonay, R., "Efficient supersonic air vehicle structural modeling for conceptual design," *12th AIAA Aviation Technology, Integration, and Operations (ATIO) Conference and 14th AIAA/ISSMO Multidisciplinary Analysis and Optimization Conference*, 2012, p. 5519.

[16] Davies, C., Stelmack, M., Zink, P. S., De La Garza, A., and Flick, P., "High fidelity MDO process development and application to fighter strike conceptual design," *12th AIAA Aviation Technology, Integration, and Operations (ATIO) Conference and 14th AIAA/ISSMO Multidisciplinary Analysis and Optimization Conference*, 2012, p. 5490.

[17] Heath, C. and Gray, J., "OpenMDAO: Framework for Flexible Multidisciplinary Design, Analysis and Optimization Methods," *Proceedings of the 53rd AIAA Structures, Structural Dynamics and Materials Conference*, Honolulu, HI, April 2012, AIAA-2012-1673.

[18] Gray, J., Moore, K. T., and Naylor, B. A., "OpenMDAO: An Open Source Framework for Multidisciplinary Analysis and Optimization," *Proceedings of the 13th AIAA/ISSMO Multidisciplinary Analysis Optimization Conference*, Fort Worth, TX, Sept. 2010, AIAA 2010-9101.

[19] Lambe, A. B. and Martins, J. R. R. A., "Extensions to the Design Structure Matrix for the Description of Multidisciplinary Design, Analysis, and Optimization Processes," *Structural and Multidisciplinary Optimization*, Vol. 46, August 2012, pp. 273–284. doi:10.1007/s00158-012-0763-y.

[20] Atmosphere, U. S., "National oceanic and atmospheric administration," *National Aeronautics and Space Administration, United States Air Force, Washington, DC*, 1976.

[21] Akima, H., "A new method of interpolation and smooth curve fitting based on local procedures," *Journal of the ACM*, Vol. 4, No. 17, 1970, pp. 589–602.

[22] van der Weide, E., Kalitzin, G., Schluter, J., and Alonso, J. J., "Unsteady Turbomachinery Computations Using Massively Parallel Platforms," *Proceedings of the 44th AIAA Aerospace Sciences Meeting and Exhibit*, Reno, NV, 2006, AIAA 2006-0421.

[23] Kenway, G. K. W., Secco, N., Martins, J. R. R. A., Mishra, A., and Duraisamy, K., "An Efficient Parallel Overset Method for Aerodynamic Shape Optimization," *Proceedings of the 58th AIAA/ASCE/AHS/ASC Structures, Structural Dynamics, and Materials Conference, AIAA SciTech Forum*, Grapevine, TX, January 2017. doi:10.2514/6.2017-0357.

[24] Secco, N. R., Jasa, J. P., Kenway, G. K. W., and Martins, J. R. R. A., "Component-based Geometry Manipulation for Aerodynamic Shape Optimization with Overset Meshes," *AIAA Journal*, 2018, (Accepted subject to revisions 2018-02-08).

[25] Bouhlel, M. A., Hwang, J. T., Bartoli, N., Lafage, R., Morlier, J., and Martins, J. R. R. A., "SMT: A surrogate Modeling Toolbox in Python," *SoftwareX*, 2018.

[26] Hwang, J. T. and Martins, J. R. R. A., "A fast-prediction surrogate model for large datasets," *Aerospace Science and Technology*, Vol. 75, April 2018, pp. 74–87. doi:10.1016/j.ast.2017.12.030.

[27] Coalson, M. S., "Development of the F110-GE-100 engine," *ASME 1984 International Gas Turbine Conference and Exhibit*, American Society of Mechanical Engineers, 1984, pp. V002T02A002–V002T02A002.

[28] Gill, P. E., Murray, W., and Saunders, M. A., "SNOPT: An SQP Algorithm for Large-Scale Constrained Optimization," *SIAM Review*, Vol. 47, No. 1, 2005, pp. 99–131. doi:10.1137/S0036144504446096.

[29] Perez, R. E., Jansen, P. W., and Martins, J. R. R. A., "pyOpt: A Python-Based Object-Oriented Framework for Nonlinear Constrained Optimization," *Structural and Multidisciplinary Optimization*, Vol. 45, No. 1, January 2012, pp. 101–118. doi:10.1007/s00158-011-0666-3.